AD

Award Number: DAMD17-99-1-9335

TITLE: Imaging of Early-Stage Breast Cancers Using Pulsed Confocal Microwave Technology

PRINCIPAL INVESTIGATOR: Milica Popovic, Ph.D.
Allen Taflove, Ph.D.

CONTRACTING ORGANIZATION: Northwestern University
Evanston, Illinois 60208-1110

REPORT DATE: May 2002

TYPE OF REPORT: Annual Summary

PREPARED FOR: U.S. Army Medical Research and Materiel Command
Fort Detrick, Maryland 21702-5012

REPORT DOCUMENTATION PAGE

Form Approved
OMB No. 074-0188

1. AGENCY USE ONLY (Leave blank)	2. REPORT DATE	3. REPORT TYPE AND DATES COVERED
	May 2002	Annual Summary (1 May 99 -30 Apr 02)

4. TITLE AND SUBTITLE
Imaging of Early-Stage Breast Cancers Using Pulsed Confocal Microwave Technology

5. FUNDING NUNUMBER
DAMD17-99-1-9335

6. AUTHOR(S)
Milica Popovic, Ph.D.
Allen Taflove, Ph.D.

7. PERFORMING ORGANIZATION NAME(S) AND ADDRESS(ES)
Northwestern University
Evanston, Illinois 60208-1110
E-Mail: poppy@ece.mcgill.ca

8. PERFORMING ORGANIZATION REPORT NUMBER

9. SPONSORING / MONITORING AGENCY NAME(S) AND ADDRESS(ES)
U.S. Army Medical Research and Materiel Command
Fort Detrick, Maryland 21702-5012

10. SPONSORING / MONITORING AGENCY REPORT NUMBER

20021113 025

11. SUPPLEMENTARY NOTES

12a. DISTRIBUTION / AVAILABILITY STATEMENT
Approved for Public Release; Distribution Unlimited

12b. DISTRIBUTION CODE

13. ABSTRACT ***(Maximum 200 Words)***

The work presented in this report is motivated by the need to calibrate a new pulsed-microwave breast tumor detection system for patient-specific skin parameters. A two-dimensional time-domain inverse-scattering algorithm based upon the finite-difference time-domain method is presented for determining the skin thickness and the relative permittivity and electric conductivity of skin in the microwave range. The algorithm traces a search trajectory in the two-dimensional parameter space. The minimal parameter estimation error along this trajectory yields a set of approximate parameter values. It is shown that the convergence of the inverse-scattering technique depends on the shape and the duration of the illuminating electromagnetic wave pulse chosen for the electrical parameter reconstruction. The time-domain nature of the inverse algorithm allows for limiting the region of inversion using causality. Thus, when the parameters of the skin are estimated, the skin thickness can be determined by comparing the measurement with a simulated all-skin response. Finally, the time-domain inverse-scattering algorithm is tested for robustness in the presence of broadband Gaussian noise. We note that the causality of the algorithm can then be exploited for the underlying breast tissue parameter recovery using the same methodology.

14. Subject Terms (keywords previously assigned to proposal abstract or terms which apply to this award)	15. NUMBER OF PAGES
Breast cancer, Inverse-Scattering, Finite Difference Time Domain (FDTD), Microwave detection, Skin electrical properties	46
	16. PRICE CODE

17. SECURITY CLASSIFICATION OF REPORT Unclassified	18. SECURITY CLASSIFICATION OF THIS PAGE Unclassified	19. SECURITY CLASSIFICATION OF ABSTRACT	20. LIMITATION OF ABSTRACT
Unclassified	Unclassified	Unclassified	Unlimited

Table of Contents

1. Introduction

The work presented in this report is motivated by the need to calibrate a new pulsed-microwave breast tumor detection system for patient-specific skin parameters. A two-dimensional time-domain inverse-scattering algorithm based upon the finite-difference time-domain method is presented for determining the skin thickness and the relative permittivity $\varepsilon_{r\text{-skin}}$ and electric conductivity σ_{skin} of skin in the microwave range. The algorithm traces a search trajectory in the two-dimensional ($\varepsilon_{r\text{-skin}}$,$\sigma_{skin}$) parameter space. The minimal parameter estimation error along this trajectory yields a set of approximate parameter values. It is shown that the convergence of the inverse-scattering technique depends on the shape and the duration of the illuminating electromagnetic wave pulse chosen for the electrical parameter reconstruction. The time-domain nature of the inverse algorithm allows for limiting the region of inversion using causality. Thus, when the parameters of the skin are estimated, the skin thickness can be determined by comparing the measurement with a simulated all-skin response. Finally, the time-domain inverse-scattering algorithm is tested for robustness in the presence of broadband Gaussian noise. We note that the causality of the algorithm can then be exploited for the underlying breast tissue parameter recovery using the same methodology.

2. Body - Description of the Research Accomplishments

Investigator's work and the research accomplishments supported by the grant from May 1999 – May 2001 have been described in the previous two annual reports submitted to US Army Medical Research and Materiel Command Office. By the end of August 2001, the investigator completed her Ph. D. requirements and was afterwards therefore no longer supported by the grant.

Cumulative research accomplishments supported by the duration of the award (May 1999 – August 2001) have been summarized in her doctoral thesis and in a manuscript prepared for submission to a major journal (*IEEE Transactions on Antennas and Propagation*). The paper was reviewed and the author is presently introducing minor modifications to comply with the reviewers' suggestions. However, this manuscript describes in detail major findings of the work supported by the award and is therefore appended to this report [Appendix A]. The manuscript first reviews the background literature on dielectric properties in the microwave range, skin thickness in the area of the human breast and numerical inverse-scattering methods. Next, calculations are presented to illustrate the importance of knowledge of the correct skin thickness for determining the time delays needed for the image-formation signal-processing algorithm tied to the microwave imaging system. Then, results are presented to show the development of two-dimensional time-domain inverse-scattering algorithm for simultaneous estimation of electrical permittivity and conductivity of the skin layer. This algorithm locates a search trajectory in the parameter space. Results are then presented which show that the convergence of the search trajectory and the convergence error depend on the shape and the duration of the impinging pulse. The estimated skin electrical parameters then permit the skin thickness to be determined by comparing the measurement with a simulated all-skin response. As the final step, the robustness of the algorithm is tested in the presence of simulated Gaussian noise for various signal-to-noise ratios. For more details and figures which illustrate major research findings, please refer to Appendix A.

3. Key Research Accomplishments

- The investigator, who has electrical engineering background, gained valuable medical insight into the anatomy of the human breast, nature of the main breast tumor categories and the related symptoms.
- Numerical models confirmed that it is important to determine accurate, local patient-specific breast thickness in order to properly calibrate the microwave breast tumor and imaging system.
- Motivated by the previously stated need for the microwave imager calibration, we have developed a two-dimensional (2-D) inverse-scattering finite-difference time-domain (FDTD) algorithm for the recovery of the electrical parameters of the skin (permittivity $\varepsilon_{r\text{-skin}}$ and electric conductivity σ_{skin}) in the microwave range. This algorithm:
  - locates a search trajectory in the ($\varepsilon_{r\text{-skin}}$,$\sigma_{skin}$) parameter space;
  - determines the square-normed error along the search trajectory;
  - locates the approximate parameter values for the minimum error.
- The algorithm was tested for several excitation waveforms.
- For each waveform under investigation, the algorithm was tested for robustness in the presence of zero-mean additive Gaussian noise for several signal-to-noise ratio values.
- The results imply that:
  - the robustness of the time-domain inverse-scattering algorithm for recovering the electrical parameters of the skin depends on the duration and shape of the excitation waveform. Specifically, of the excitations considered, a 10-ps differentiated Gaussian pulse provides superior robustness, even relative to the ramp signal having the same rise-time, if the time window used for the inverse-scattering procedure contained the entire scattered waveform.
  - The use of a time-linear excitation yields a linear search trajectory in the parameter space ($\varepsilon_{r\text{-skin}}$,$\sigma_{skin}$).
  - Proper combination of time-linear and short bipolar pulse excitation data can yield an efficient and robust search strategy.
- By exploiting causality, after skin electrical parameters are determined, skin thickness can be estimated by comparing the measurement and the simulated all-skin response.
- The same methodology can then be employed to determine the electrical parameters of the underlying breast tissue.

4. Reportable outcomes

In this section, the investigator reports the outcomes which were supported by the award for the entire award period (May 1999 – August 2001). The outcomes which were appended in the previous reports are only listed, and those which date from after the last annual report are included in the appendices as noted.

DOCTORAL THESIS

M. Popovic, "Microwave Imaging of Breast Tissues", published March 13, 2002, United States Copyright Office, Registration Number TX 5-498-417, USA. (Please see Appendix C for the front page.)

JOURNAL PAPERS

M. Popovic, A. Taflove, "2-D FDTD Inverse-Scattering Scheme for Determination of Breast Skin Properties at Microwave Frequencies", *manuscript submitted to IEEE Trans. On Antennas and Propagation, August 2001. Manuscript is currently under revision in order to comply with the reviewers' comments prior to resubmission.* [Appendix A]

REFEREED CONFERENCE PROCEEDINGS PAPERS

M. Popovic and A. Taflove, "Skin Thickness and Dielectric Parameter Evaluation in the Microwave Range Using an FDTD Inverse-Scattering Technique", *Proceedings on 2001 URSI International Symposium on Electromagnetic Theory*, Victoria, Canada. May 13-17, 2001.

ABSTRACTS AND PRESENTATIONS

M. Popovic and A. Taflove, "Noninvasive Measurement of Breast Skin Properties in the Microwave Range: Efficiency Improvement of the 2-D FDTD Inverse-Scattering Scheme", The Tenth Biennial IEEE Conference on Electromagnetic Field Computation, Perugia, Italy, June 16-19, 2002. [Appendix B]

M. Popovic and A. Taflove, "2-D FDTD Inverse-Scattering Scheme for Determining Microwave Breast Skin Properties: the Results and the Implied Optimization Options", The Bioelectromagnetics Society 24th Annual Meeting, Quebec City, Canada, June 23-27, 2002. [Appendix B]

M. Popovic and A. Taflove, "Skin Thickness and Dielectric Parameter Evaluation in the Microwave Range Using an FDTD Inverse-Scattering Technique", 2001 URSI International Symposium on Electromagnetic Theory, Victoria, Canada. May 13-17, 2001.

M. Popovic and A. Taflove, "Time Domain Inverse-Scattering Technique for Obtaining Microwave Properties of Near-Surface Body Tissues", Progress in Electromagnetics Research Symposium (PIERS), July 5-14, 2000, Cambridge, Massachusetts, USA, pp. 550.

M. Popovic and A. Taflove, "Obtaining Microwave Properties of Near-Surface Body Tissues Using 2-D FDTD Inverse-Scattering Technique", Bioelectromagnetics Society (BEMS) 2000 Twenty-Second Annual Meeting, June 11-16, 2000, Munich, Germany, pp.23.

S. C. Hagness, M. Popovic, A. Taflove and Jack E. Bridges, "An Image Reconstruction Algorithm for Ultrawideband Microwave Radar Technology Applied to Breast Cancer Detection", 1999 IEEE AP-S International Symposium and USNC/URSI National Radio Science Meeting, July 11-16, 1999, Orlando, Florida, USA.

DEGREES OBTAINED

The applicant defended her Doctoral work in July 2002, and completed the requirements for the Ph.D. in August 2002 [Appendix C], obtaining the official diploma in December 2002.

AWARDS

- May 1999: Award for one of the two best poster presentations, ECE Research and Industry Fair, ECE Department, Northwestern University.

- BEMS 2000 Twenty-second Annual Meeting, *EMF Therapeutics Clinical Application Award,* June 11-16, Munich, Germany.

EMPLOYMENT AND RESEARCH OPPORTUNITIES

The doctoral research funded by the award was referred to in over ten applications for academic positions across North America. One of the interviews led to employment of the investigator as an assistant professor with the Department Electrical and Computer Engineering at McGill University, Montreal, Canada, beginning September 2001, to the present date. (Please refer to Appendix D for a copy of the appointment letter from the Academic Vice-Principal.)

As an assistant professor and a researcher, the investigator applied for funding from both federal and provincial sources in Canada in order to continue the research started under the Department of Defense pre-doctoral grant.

Received funding:

- Natural Sciences and Engineering Research Council of Canada (NSERC) – Individual Research Grant (3-year program; level received: approximately $42,000 CDN / year);
- Internal Research Grants Office Funding – McGill University: Individual New Researcher Grant, $17,500 CDN, one-time grant.

Applied for and pending funding:

- Fonds pour la Formation de Chercheurs et l'aide a la Recherche (FCAR) – Quebec:
  - Programmes destinees aux nouveaux chercheurs – requested $15,000 CDN;
  - Programme stratégique de professeurs-chercheurs réservé aux universities – supplies the salary of the applicant to the university department and reduces teaching load in favor of the research time.

5. Conclusions

In this report, we presented the research conducted to investigate possibilities of non-invasive determination of near-surface breast tissue electrical properties in order to aid the patient-specific calibration of the microwave tumor detection and imaging device. When a layer of materials (tissues) is excited with a signal, information about the tissue electrical properties is hidden in the backscattered signal data. A 2-D FDTD inverse-scattering algorithm was developed to show that non-invasive measurement of near-surface tissue properties depends heavily on the shape and the duration of the impinging signal. Moreover, studies suggest that usage of a short, bipolar excitation can yield an accurate estimate of the skin electrical properties even in the presence of high-level random Gaussian noise.

A logical near-term extension of this work is to construct an additional software-element which would use the same technique to obtain the electrical properties of the breast tissue underlying the skin after first determining the skin thickness and its electrical properties. A second extension of this technique would be to exploit its potential multidimensional search capabilities to determine the frequency dispersion of the electrical properties of the skin and the underlying breast tissues. Finally, a long-term goal of this work would be extension of the verified 2-D algorithm to three dimensions.

REFERENCES

[1] S. C. Hagness, A. Taflove and J.E. Bridges, "Two-Dimensional FDTD Analysis of a Pulsed Microwave Confocal System for Breast Cancer Detection: Fixed-Focus and Antenna-Array Sensors", *IEEE Trans. Biomedical Eng.*,vol. 45, no. 12, Dec. 1998, pp. 1470-1479.

[2] E. C. Fear and M. A. Stuchly, "Microwave Detection of Breast Cancer", *IEEE Trans. Microwave Theory and Techniques,* vol 48, no. 11, Nov. 2000, pp. 1470-1479.

[3] Jr. T. L. Pope, M. E. Read, T. Medsker, A. J.. Buschi and A. N. Brenbridge, "Breast skin thickness: normal range and causes of thickening shown on film-screen mammography", *J. Canadian Assoc. of Radiologists,* vol. 35, Dec. 1984, pp. 365-693.

[4] K. R. Umashankar, S. Chaudhuri and A. Taflove, "Finite-difference time-domain formulation of an inverse-scattering scheme for remote sensing of inhomogeneous lossy layered media", *J. Electromagn. Waves Apps.*, vol. 8, pp. 489-509, 1994.

[5] M. Popovic and A. Taflove, Annual Report May 2000, NTIS, document reference number: AD385306.

[6] A. S. Breathnach, *An Atlas of the Ultrastructure of Human Skin*, J. & A. Churchill, London, 1971.

[7] R. M. Marks, S. P. Barton and C. Edwards, eds., *The Physical Nature of the Skin*, MTP Press Ltd, Lancaster, England,1988. pp. 2271-2293.

[8] D. Gilligan, J. A. Hendry and J. R. Yarnold, "The use of ultrasound to measure breast thickness to select electron energies for breast boost therapy", *Radiotherapy and Oncology*, Vol. 32, 1994. pp 265-273.

[9] J. P. Grant, R. N. Clarke, G. T. Symm and N. M Spyrou, "*In vivo* dielectric properties of human skin from 50 MHz to 2.0 GHz", *Physics in Medicine and Biology*, Vol. 33, No. 5, 1998, pp. 607-612.

[10] H. I. Libshitz, E. D. Montague and D. D. Paulus, Jr.,"Skin thickness in the therapeutically irradiated breast", *American Journal of Roentgenology*, Vol. 130, 1978, pp. 345-347.

[11] G. T. Mogavero, E. K. Fishman and J. E. Kuhlman, "Inflammatory breast cancer: {CT} evaluation", *Clinical Imaging*, Vol. 16, 1992, pp. 183-186.

[12] M. Olenius and O. Johansson, "Variations in epidermal thickness in expanded human breast skin", *Scandinavian Journal of Plastic and Reconstructive and Hand Surgery*, Vol. 29, 1995, pp. 15-20.

[13] D. Sulitzeanu, "Markers in breast cancer", *Israel Journal of Medical Science*, 1981, pp. 865-868.

[14] T. Tamura, M. Tenhunen, T. Lahtinen and H. P. Schwan, "Modelling of the dielectric properties of normal and irradiated skin", *Physics in Medicine and Biology*, Vol. 39, 1994, pp. 927-936.

[15] S. A. Wilson and E. J. Adam and A. K. Tucker, "Patterns of breast skin thickness in normal mammograms", *Clinical Radiology*, Vol. 33, 1982, pp. 691-693.

Appendix A

Manuscript submitted to *IEEE Antennas and Propagation*, August 2002.
The manuscript is currently under revision, introducing minor changes to comply with the reviewers' comments prior to resubmission.

2-D FDTD Inverse-Scattering Scheme for Determination of Breast Skin Properties at Microwave Frequencies

M. Popović, *Student Member, IEEE*

and A. Taflove, *Fellow, IEEE*

M. Popović is with the Department of Electrical and Computer Engineering, McGill University, McConnell Engineering Building, 3480 University Street, Montreal, Quebec, Canada H3A-2A7.

A. Taflove is with the Department of Electrical and Computer Engineering, McCormick School of Engineering, Northwestern University, 2145 Sheridan Road, Evanston, IL 60208 USA.

This work was sponsored by the United States Department of Defense pre-doctoral grant, under Army Award number DAMD17-99-1-9335.

August 28, 2001

Abstract

The work presented in this paper is motivated by the need to calibrate a new pulsed-microwave breast tumor detection system for patient-specific skin parameters. A two-dimensional time-domain inverse-scattering algorithm based upon the FDTD method is presented for determining the skin thickness and the relative permittivity ε_{r-skin} and electric conductivity σ_{skin} in the microwave range. The algorithm traces a search trajectory in the $(\varepsilon_{r-skin}, \sigma_{skin})$ parameter space. The minimal parameter estimation error along this trajectory yields a set of approximate parameter values. It is shown that the convergence of the inverse-scattering technique depends on the shape and the duration of the illuminating electromagnetic wave pulse chosen for the electrical parameter reconstruction. The time-domain nature of the inverse algorithm allows for limiting the region of inversion using causality. Thus, when the parameters of the skin are estimated, the skin thickness can be determined by comparing the measurement with a simulated all-skin response. Finally, the time-domain inverse-scattering algorithm is tested for robustness in the presence of broadband Gaussian noise.

Keywords

Two-dimensional, FDTD, inverse-scattering, breast skin

I. Introduction

The investigations presented here are motivated by the development of a new ultra-wideband confocal microwave technology to detect and image early-stage breast cancers [1], [2], [3], [4], [5], [6], [7], [8], [9], [10], [11], [12] . The new technology exploits the dielectric property contrast between normal breast tissues and malignant tumors at microwave frequencies. Here, microwave imaging is performed by a planar antenna array contacting only one side of the breast. The antenna array elements collect impulsive backscattered signals, which are digitally delayed to achieve coherent summation at the site of a potential tumor. This scheme depends upon knowledge of the average dielectric properties of the local breast tissues. Patient-specific calibration of the microwave imager requires knowledge of these properties.

In the present research, a time-domain inverse-scattering technique is studied to measure the skin thickness and dielectric parameters in the area of the human breast. This study is motivated by several well-documented findings [13], [14], [15], [16]. Skin thickness varies from patient to patient, and also with location on the body of an individual patient. A

number of factors can cause thickening of mammary skin. Although this study is primarily motivated by assisting patient-specific calibration of the microwave breast cancer imaging system, determining breast skin thickness can also help to diagnose possible pathologies in the underlying tissue and in the patient in general.

This paper first reviews the background literature on dielectric properties in the microwave range, skin thickness in the area of the human breast, and numerical inverse-scattering methods. Next, calculations are presented to illustrate the importance of knowledge of the correct skin thickness for determining the time delays needed for the image-formation signal-processing algorithm. Then, results are presented to show the development of a two-dimensional time-domain inverse-scattering algorithm for simultaneous estimation of electrical permittivity ε_{r-skin} and conductivity σ_{skin} of the skin layer. This algorithm locates a search trajectory in the (ε_{r-skin}, σ_{skin}) parameter space. Results are then presented which show that the convergence of the search trajectory and the convergence error depends on the shape and the duration of the impinging pulse. This convergence then permits the skin thickness to be determined by comparing the measurement with a simulated all-skin response. Finally, the robustness of the algorithm is tested in the presence of Gaussian noise for various signal-to-noise ratios.

II. Background

A. Dielectric Properties of Breast Tissues in the Microwave Range

Extensive dielectric measurements up to 3 GHz of both normal and malignant human breast tissues have been reported in the literature [17], [18], [19], [20], [21]. At 6 GHz, normal breast tissue dielectric properties are similar to those of fat and vary in an approximate $\pm 10\%$ range about $\varepsilon_{r-breast} = 9$ for the permittivity and $\sigma_{breast} = 0.4\ S/m$ for the conductivity. Malignant tumor dielectric properties are similar to those of muscle. They have nominal values of $\varepsilon_{r-tumor} = 50$ and $\sigma_{tumor} = 7\ S/m$. This dielectric contrast causes malignant tumors to have significantly larger microwave backscattering cross sections relative to normal tissues of comparable size and geometry. For breast skin tissue, the values found in the literature are approximately $\varepsilon_{r-skin} = 36$ and $\sigma_{skin} = 4\ S/m$ in the microwave frequency range [19], [20], [21], [22].

B. Skin Properties and Thickness in the Area of the Human Breast

The literature offers several studies on skin thickness in the area of the human breast. A comprehensive normal range of breast skin thickness and the causes of thickening shown on film-screen mammography is given in [16]. Breast skin thickness ranges from 0.7 mm – 2.7 mm depending upon the location. Specifically, the inferior skin has maximum thickness (mean value = 1.7 mm); the medial and superior skin thicknesses both average 1.5 mm; and the lateral skin has minimum thickness (mean value = 1.3 mm).

The reported causes of mammary skin thickening are commonly categorized by their local or generalized nature. The localized causes can be carcinoma, inflammation, trauma, fat necrosis, post-biopsy and dermatological conditions. The generalized causes found in the literature are breast cancer, Hodgkin's disease, reticulum cell sarcoma, metastatic disease, radiation therapy, inflammation, surgery, primary skin disorders, anasarca and any cause of lymphatic obstruction. Therefore, careful monitoring of breast skin thickness can also be used as a pre-diagnostic tool of the underlying tissue pathologies or health concerns of the patient in general.

C. Numerical Inverse-Scattering Methods

Numerical inverse-scattering studies found in the literature are based on either frequency- or time-domain approaches. With frequency-domain algorithms, the interaction of the entire medium with the incident field is considered simultaneously [23], [24], [25], [26]. For a general, lossy inhomogeneous medium this can result in a very large number of unknown parameters. In contrast, time-domain approaches can exploit causality to limit the region of inversion, potentially reducing the number of unknowns.

Time-domain inverse-scattering problems somewhat related to the present study commonly appear in the area of geoscience and remote sensing [27], [28], [29]. In such problems, ground-penetrating radar (GPR) is used to obtain information on subsurface features from data collected over the surface. Signal-processing algorithms, including those based on FDTD [27], [28], can be used for target reconstruction. Global inversion techniques have emerged involving the neural network method [28] and the use of genetic algorithms [29]. These algorithms, based on stochastic strategies, offer advantages relative to local in-

version algorithms including strong search ability, simplicity, robustness, and insensitivity to ill-posedness. However, they require a high number of function evaluations.

More relevant to the present work is the FDTD / nonlinear optimization techniques of [30] and [31]. Reference [30] reported a one-dimensional FDTD formulation of an inverse-scattering scheme for remote sensing of inhomogeneous lossy layered media. Here, a layer-stripping procedure was used to simultaneously recover the conductivity and permittivity profiles. This work assumed an normally incident plane wave pulse and zero noise present on the received pulse.

Reference [31] reported a two-dimensional FDTD inverse-scattering scheme for remote sensing of the shape of conducting and dielectric targets. With this technique, as the illuminating wavefront sweeps across the target, causality is exploited to reconstruct the actual target surface contour in a sequential and cumulative manner. To test the complexity of a recoverable structure, a plane-wave-illuminated dielectric target with reentrant features was reconstructed from a single-point observation. Numerical experiments tested the performance of the algorithm in the presence of noise and demonstrated a promising degree of robustness.

In the present work, the one-dimensional inversion technique of [30] is extended to two-dimensional illumination of a layered medium by an infinite monopole source located at the surface. Both the time waveform and the duration of the illuminating pulse are studied to explore optimization of the convergence of the inverse-scattering technique. Further, the robustness of the technique in the presence of noise is examined.

III. Single-Parameter Reconstruction of Skin Dielectric Properties

A. Rationale and Motivation

Fig. 1 shows a simplified 2-D geometry of the 17-element microwave antenna array system adjacent to the breast skin, underlying breast tissue, and a $5-mm$ spherical tumor in the breast tissue 3 cm below the skin surface on the central axis of the sensing antenna array. Signals received by each antenna element of the synthetic-aperture array are shifted in time for coherent summation. We use values of $\varepsilon_{r-skin} = 36$, $\varepsilon_{r-breast} = 9$ and principles of geometrical optics to calculate theoretical time delays between the transmitted signal

and the backscatter from the tumor location for each element of the antenna array of Fig. 1. Fig. 2 graphs calculated time delays for the extreme values of the reported skin thickness range. We note that the range of variation (i.e., uncertainty) in these delays is comparable to the difference in time delays required for coherent addition for two adjacent antenna elements for each thickness value considered. This demonstrates that an incorrect assumption of skin thickness can lead to incoherent summation of the individual received signals. Additional calculations show that, due to the relatively thin skin layer, the effect of the variation in ε_{r-skin} on the variation in the calculated time delays is not as pronounced. Overall, the result presented in Fig. 2 implies that we require a patient-specific calibration of the confocal microwave imager for breast skin thickness and its dielectric parameters.

B. Basic Technique

This work focuses on the development of a time-domain inverse-scattering algorithm that permits a noninvasive measurement of the near-surface dielectric parameters of a lossy layered half-space. The new algorithm extends the iterative technique of [30] to the case of a 2-D half-space excited at its surface by an infinitely long monopole. The principal logic of this scheme is shown in Fig. 3.

Based on an initial guess for a set of dielectric parameters (ε_r, σ), the FDTD code computes a trial backscattered time waveform. The algorithm compares a trial signal with the measured signal and calculates the energy-normed error. Based on this error, the dielectric parameters are perturbed by a gradient-based nonlinear optimization routine, and the FDTD code computes a new trial backscattered signal based on this new guess for (ε_r, σ). This process is repeated with varying ε_r and σ perturbations as needed.

There are two ways to exit the iterative loop of Fig. 3. For exit 1, the energy-normed error decreases below a pre-determined threshold value. For exit 2, the error remains above the threshold but the estimated ε_r and σ parameters oscillate within a narrow band of values a pre-determined number of times. Both of these exit criteria are chosen according to physical meaningfulness and to limitations imposed by available computational resources.

C. Results in the Absence of Noise

Here, we illustrate the convergence properties of the time-domain inverse-scattering algorithm of Fig. 3 for a skin half-space with only one unknown parameter, ε_{r-skin} or σ_{skin}. A 120-ps (1/e full-width) differentiated Gaussian pulse is used as the excitation waveform.

In Case 1 (Fig. 4(a)), we fix the value of σ_{skin} at the correct value of 4 S/m while iterating for ε_{r-skin}. Here, the FDTD code computes the backscattered signal for a trial value of ε_{r-skin}, compares it with the reference backscattered signal obtained for the correct value of ε_{r-skin}, and calculates the energy-normed error. Based on this error, ε_{r-skin} is perturbed, and the FDTD code computes the backscattered signal for this new guess for the permittivity. This is repeated until one of the criteria for exiting the iterative process is met. Sample results are shown for two initial guesses of ε_{r-skin}, 99 and 150.

In Case 2 (Fig. 4(b)), we fix the value of ε_{r-skin} at the correct value of 36 while iterating for σ_{skin}. Sample results are shown for two initial guesses for σ_{skin}, 19 S/m and 20 S/m. In these and similar simulations, we have found a robust convergence for ε_{r-skin} and σ_{skin} in the absence of noise for a variety of parameter perturbation increments.

IV. Two-Parameter Reconstruction of Skin Dielectric Properties

A. Methods

This section describes an optimization scheme which allows simultaneous recovery of the permittivity and conductivity of the skin. This scheme generates a search trajectory in the (ε_{r-skin}, σ_{skin}) space that ideally converges to the reference values of these parameters.

The search trajectory is generated in two possible ways:

1. A trial value of σ_{skin} is assumed and a series of FDTD forward-scattering runs is conducted to find a corresponding value of ε_{r-skin} which minimizes the energy-normed error relative to the measured backscattered waveform. This procedure is then repeated for a sequence of trial values of σ_{skin} which vary uniformly in equal increments within a $\pm 50\%$ range about the nominal value reported in the literature.

2. A trial value of ε_{r-skin} is assumed and a series of FDTD forward-scattering runs is conducted to find a corresponding value of σ_{skin} which minimizes the energy-normed error relative to the measured backscattered waveform. This procedure is then repeated for a

sequence of trial values of ε_{r-skin} which vary uniformly in equal increments within a $\pm 50\%$ range about the nominal value reported in the literature.

We here introduce the excitation waveforms used in our investigations. The results section will show that the search trajectory in the (ε_r, σ) space depends strongly on the signal shape and duration of the excitation waveform. The three E_z-field excitation waveforms used for the dielectric parameter reconstruction are as follows: (a) $120-ps$ differentiated Gaussian pulse; (b) $10-ps$ differentiated Gaussian pulse with a $5-ps$ rise-time; and (c) $5-ps$ rise time ramp which has the same maximum as the peak value of the $10-ps$ differentiated Gaussian pulse.

It is important to note the following. The inverse-scattering algorithm processes only a time window T_{window} within which it compares the trial and measured signals. For breast-skin parameter recovery, it is critical that T_{window} be small enough to avoid wave reflection from the underlying skin-breast interface which corrupts the received signal. However, T_{window} must be large enough to allow the measured backscattered pulse to contain meaningful information concerning the skin electrical parameters. This, in turn, means that only a part of the measured backscattered waveform might be usable for accurately generating a trajectory in the (ε_{r-skin}, σ_{skin}) space. For example, in the next section, we will see that, for the $120-ps$ differentiated Gaussian pulse excitation case, only the leading edge of the measured backscattered pulse is used in the reconstruction. Conversely, the entire measured backscattered pulse is used for the $10-ps$ differentiated Gaussian pulse excitation case. Results will illustrate the significant consequences that this has on the calculated trajectory in the (ε_{r-skin}, σ_{skin}) space.

B. Results in the Absence of Noise

B.1 ε_{r-skin} Reconstruction with Trial Values of σ_{skin}

This section reports results for the inverse-scattering algorithm iterating for ε_{r-skin} using a range of trial values of σ_{skin} varying $\pm 50\%$ around the reference value of $\sigma_{skin} = 4\ S/m$. In all simulations, the time step used in the FDTD code is $\Delta t = 0.33356\ ps$.

Fig. 5(a) depicts the resulting trajectory in the (ε_{r-skin}, σ_{skin}) space for the $120-ps$ differentiated Gaussian pulse excitation and $T_{window} = 400\Delta t$. This trajectory passes

through the reference value $\varepsilon_{r-skin} = 36$. Fig. 5(a) also shows the large error made in the ε_{r-skin} recovery if $T_{window} = 600\Delta t$, which is large enough to include the unwanted reflection from the underlying skin – breast tissue interface. Fig. 5(b) graphs the error for T_{window} for each value in the trial σ_{skin} range for its corresponding estimated ε_{r-skin} of Fig. 5(a). Fig. 5(b) shows that the error function for ε_{r-skin} recovery using trial values of σ_{skin} suffers from local minima, and thus cannot be used as a search criterion along the trajectory in the $(\varepsilon_{r-skin}, \sigma_{skin})$ space. Similar results were observed for the 10-ps differentiated Gaussian pulse and 5-ps rise-time ramp excitation.

B.2 σ_{skin} Reconstruction with Trial Values of ε_{r-skin}

This section reports results for the inverse-scattering algorithm iterating for σ_{skin} using a range of trial values of ε_{r-skin} varying $\pm 50\%$ around the reference value of $\varepsilon_{r-skin} = 36$ S/m. In all simulations, the time step used in the FDTD code is $\Delta t = 0.33356\ ps$.

Results for the excitation signal waveforms under investigation are shown in Figs. 6, 7 and 8. For the $120 - ps$ differentiated Gaussian pulse (Fig. 6) and the $5 - ps$ rise-time ramp (Fig. 7), T_{window} includes only the leading edge of the backscattered pulse waveform. This yields in Fig. 6(a) and Fig. 7(a) linear search trajectories in the $(\varepsilon_{r-skin}, \sigma_{skin})$ space. For both of these excitations, Fig. 6(b) and Fig 7(b) show a broad minimum of the error along the search trajectory as a function of the estimated σ_{skin} value. This minimum is approximately centered at the location of the assumed reference values of ε_{r-skin} and σ_{skin}, implying that minimizing the error could be used as a search criterion along the trajectory in the $(\varepsilon_{r-skin}, \sigma_{skin})$ space. However, the broad error minimum suggests sensitivity of the skin dielectric parameter recovery in the presence of noise.

Fig. 8(a) graphs the search trajectory in the $(\varepsilon_{r-skin}, \sigma_{skin})$ space obtained for the $10-ps$ differentiated Gaussian pulse excitation. Here, T_{window} includes the entire backscattered pulse waveform, and the search trajectory shows a parabolic behavior. We note a sharp null of the error along the search trajectory at the location of the assumed reference values of the skin dielectric parameters, which suggests robustness of parameter recovery in the presence of noise. This is explored next.

C. *Results in the Presence of Zero-Mean Gaussian Noise*

We now test the robustness of the inverse-scattering scheme of the previous section by adding zero-mean Gaussian noise to the simulated measured backscattered signals. The signal-to-noise (S/N) ratio is defined by $20\ log_{10}(Signal_{MAX}/Noise_{SD})$, where $Signal_{MAX}$ is the peak value of the noiseless backscattered waveform and $Noise_{SD}$ is the standard deviation of the zero-mean Gaussian noise.

This section presents results for noisy backscattered signals resulting from the $10 - ps$ differentiated Gaussian pulse excitation. Individual search trajectories in the (ε_{r-skin}, σ_{skin}) space are generated for five independent noise samples added to the backscattered signal for S/N ratios of 20 and 40 dB. Then, for each S/N level, the five data sets are averaged before input to the inverse-scattering algorithm to yield a final search trajectory. The latter procedure simulates the "boxcar integration" often used as a technique for measuring signals contaminated with zero-mean noise wherein multiple measurements are averaged to enhance the deterministic signal. For all results shown, $T_{window} = 80\ \Delta t$, where $\Delta t = 0.33356\ ps$. Figs. 9(a) and 10(a) show the generated search trajectories in the (ε_{r-skin}, σ_{skin}) space for each noisy and the averaged backscattered waveform for $S/N = 20$ and 40 dB, respectively. As expected, for the higher S/N ratio, we observe a smaller deviation of the individual trajectories from the trajectory obtained using the averaged backscattered signal.

More importantly, however, Figs. 9 and 10 show that the corresponding error along the search trajectory as a function of the estimated σ_{skin} exhibits a sharp null at the correct value of ε_{r-skin}, 36, even for the lower value of S/N. This unambiguous indication of the correct value of ε_{r-skin} despite a noisy background is crucial in the determination of the skin thickness, to be discussed next.

V. Determining Skin Thickness

We now briefly describe how we can estimate the breast skin thickness once the patient-specific value for ε_{r-skin} is determined. Note that this procedure is relatively insensitive to σ_{skin}. Here, the excitation signal shape and duration is much less critical than before.

Due to the dielectric contrast between the skin and the underlying breast tissue, the

propagating pulse reflects off the skin - breast tissue interface. By comparing the measured response for the finite skin-thickness case with an FDTD simulation which assumes a homogeneous skin half-space characterized by the ε_{r-skin} determined previously, the observed time of the first reflection yields the data required to determine the skin thickness.

To illustrate this strategy, Fig. 11 graphs the results of four test cases for an assumed $60-ps$ differentiated Gaussian pulse excitation wherein measured backscattered waveforms for skin thicknesses of 0.6, 1.2, 1.8 and 2.4 mm and $\varepsilon_{r-skin} = 36$ are simulated using 2-D FDTD models. These waveforms are subtracted from the FDTD-calculated backscattered response for the corresponding skin half-space. Then, the estimated time delay of the peak value of the difference signal with respect to the peak of the skin half-space response is used to estimate the skin thickness. The resulting breast skin thickness values obtained in this manner are $0.51, 1.25, 1.85$ and 2.45 mm, respectively.

VI. Discussion

A. Impact of the Excitation Signal Shape and Duration Upon the Robustness of the Inverse-Scattering Algorithm

The results of the previous sections show that the robustness of the time-domain inverse-scattering algorithm for recovery of ε_{r-skin} and σ_{skin} depends on the duration and shape of the excitation waveform. Specifically, of the excitations considered, the $10-ps$ differentiated Gaussian pulse provides superior robustness, even relative to the ramp signal having the same rise-time, if T_{window} includes the entire backscattered waveform due to the differentiated Gaussian pulse. Apparently, a bipolar excitation delivers more information to the proposed inverse-scattering algorithm about the signal-path propagation medium than a comparably fast unipolar excitation. The sharp error null consistently obtained along the search generated trajectory in the $(\varepsilon_{r-skin}, \sigma_{skin})$ space for the $10-ps$ differentiated Gaussian pulse excitation, even in the presence of significant levels of zero-mean Gaussian noise, clearly illustrates this point. Signal-to-noise ratios as low as 20 dB are adequate for reliable recovery of the skin permittivity using this excitation.

B. Linearity of Estimated σ_{skin} vs. ε_{r-skin} in the Case of Time-Linear Excitations

In the previous sections, we observed that the search trajectory in the $(\varepsilon_{r-skin}, \sigma_{skin})$ space is a straight line for cases where the leading edge of the $120-ps$ differentiated Gaussian pulse or the $5-ps$ rise-time ramp excitation was used for simulation of backscattered signals and parameter reconstruction. This was observed even in the presence of zero-mean Gaussian noise. In this section, we analyze the connection between the linear time-dependence of the excitation pulse and the linearity of the generated search trajectory.

We begin the analysis with Ampere's law in three dimensions for linear, isotropic, nondispersive, lossy materials:

$$\nabla \times \vec{H} = (\vec{J}_{source} + \sigma\vec{E}) + \varepsilon \cdot \frac{\partial \vec{E}}{\partial t} \tag{1}$$

Here, $\vec{H}$ is the magnetic field (A/m); $\vec{E}$ is the electric field (V/m); $\vec{J}_{source}$ is an independent source current density (A/m^2); σ is the conductivity (S/m); and $\varepsilon = \varepsilon_0\varepsilon_r$ is the electrical permittivity (F/m), the product of relative permittivity ε_r with the free-space permittivity $\varepsilon_0 = 8.854 \times 10^{-12}\ F/m$.

In two dimensions and in the absence of independent current sources, Equation 1 can be reduced to the TM-mode scalar equation involving Cartesian components of the field vectors:

$$\frac{\partial H_y}{\partial t} - \frac{\partial H_x}{\partial t} = \sigma E_z + \varepsilon \cdot \frac{\partial E_z}{\partial t} \tag{2}$$

This equation governs both the measured backscattered signal and the FDTD-computed trial backscattered signal:

$$\frac{\partial H_{y,M}}{\partial t} - \frac{\partial H_{x,M}}{\partial t} = \sigma_M E_{z,M} + \varepsilon_M \cdot \frac{\partial E_{z,M}}{\partial t} \tag{3}$$

$$\frac{\partial H_{y,T}}{\partial t} - \frac{\partial H_{x,T}}{\partial t} = \sigma_T E_{z,T} + \varepsilon_T \cdot \frac{\partial E_{z,T}}{\partial t} \tag{4}$$

where the subscript M refers to measured signal variables and the subscript T refers to trial signal variables. The excitation for both the measured and the trial pulse is the same and a linear function of time:

$$E_{z,M} = E_{z,T} = at + b \tag{5}$$

and

$$\frac{\partial E_{z,M}}{\partial t} = \frac{\partial E_{z,T}}{\partial t} = a \tag{6}$$

where a and b are constants with appropriate units.

The proposed inverse-scattering iterative scheme computes the error based on energy difference. In essence, the iterative process attempts to minimize the following difference:

$$[(\frac{\partial H_{y,M}}{\partial t} - \frac{\partial H_{x,M}}{\partial t}) - (\frac{\partial H_{y,T}}{\partial t} - \frac{\partial H_{x,T}}{\partial t})]^2 \longrightarrow 0 \tag{7}$$

In order for this difference to reach zero, while observing Equations 2, 4, 5 and 6, the following condition must be fulfilled:

$$[(\sigma_M \cdot (at+b) + \varepsilon_M \cdot a) - (\sigma_T \cdot (at+b) + \varepsilon_T \cdot a)]^2 = 0 \tag{8}$$

Clearly, Equation 8 is satisfied when the trial values of parameters are equal to the measured parameter values, i.e., when $\varepsilon_T = \varepsilon_M$ and $\sigma_T = \sigma_M$. However, Equation 8 is satisfied also for the following condition:

$$\varepsilon_T = -\frac{(at+b)}{a} \cdot \sigma_T - [\sigma_T \cdot \frac{(at+b)}{a} + \varepsilon_M] \tag{9}$$

Therefore, the minimal error condition of Equation 8 and the final Equation 9 tells us that linear relation between ε_T and σ_T with appropriate constants is a sufficient condition for reconstruction of ε and σ parameters by the proposed inverse-scattering scheme when the excitation signal is a linear function of time. This was observed even for the noise study in the case of the the linear, 5-ps ramp signal excitation. The potential benefit of the demonstrated linearity of the generated search trajectory in the $(\varepsilon_{r-skin}, \sigma_{skin})$ space is as follows: linear excitation can be used for two trial ε_{r-skin} values, and the rest of the values along the anticipated linear $(\varepsilon_{r-skin}, \sigma_{skin})$ trajectory can be obtained by interpolation or extrapolation. Then, error values for the sets of $(\varepsilon_{r-skin}, \sigma_{skin})$ obtained by this means can be tested with the noise-robust $10-ps$ differentiated Gaussian pulse excitation. This would significantly decrease the computational cost of the dielectric recovery procedure.

VII. Conclusion

This work presented investigations of a novel time-domain inverse-scattering technique that has promise for permitting calibration of the pulsed confocal microwave imager for human breast cancers. The new technique is based upon the use of an FDTD forward-scattering program element embedded within a numerical feedback loop containing a non-linear optimization routine. A systematic parameter-perturbation strategy is adopted to

permit searching of a multidimensional parameter space for the electrical properties of the breast skin.

There are two significant findings of this work. First, the use of a time-linear (ramp) excitation yields a linear search trajectory in $(\varepsilon_{r-skin}, \sigma_{skin})$ space. Second, the use of a short bipolar excitation signal provides a sharp null of the energy-normed error along the search trajectory even when the backscattered signal is contaminated with a significant level of additive zero-mean Gaussian noise. Proper combination of time-linear and short bipolar pulse excitation data can yield an efficient and robust search strategy.

A logical near-term extension of this work is to construct an additional software-element which would use the same technique to obtain the electrical properties of the breast tissue underlying the skin after first determining the skin thickness, permittivity and conductivity. A second extension of this technique would be to exploit its potential multidimensional search capabilities to determine the frequency dispersion of the electrical properties of the skin and the underlying breast tissues.

VIII. Acknowledgment

This work was sponsored by the United States Department of Defense pre-doctoral grant, under Army Award number DAMD17-99-1-9335.

The authors would like to thank Cray Research for their computational resources.

References

[1] E. C. Fear and M. A. Stuchly, "Microwave detection of breast cancer," *IEEE Transactions on Microwave Theory and Techniques*, vol. 48, no. 11, pp. 1854–63, Nov. 2000.

[2] S. C. Hagness, A. Taflove, and J. E. Bridges, "Two-dimensional FDTD analysis of a pulsed microwave confocal system for breast cancer detection: fixed-focus and antenna-array sensors," *IEEE Transactions on Biomedical Engineering*, vol. 45, no. 12, pp. 1470–1479, Dec. 1998.

[3] S. C. Hagness, A. Taflove, and J. E. Bridges, "Three-dimensional FDTD analysis of a pulsed microwave confocal system for breast cancer detection: design of an antenna-array element," *IEEE Transactions on Antennas and Propagation*, vol. 47, no. 5, pp. 783–791, May 1999.

[4] X. Li and S. Hagness, "A conforcal microwave imaging algorithm for breast cancer detection," *IEEE Microwave and Wireless Components Letters*, vol. 11, no. 3, pp. 130–132, Mar. 2001.

[5] P. M. Meaney, M. W. Fanning, D. Li, S. P. Poplack, and K. D. Paulsen, "A clinical prototype for active microwave imaging of the breast," *Microwave Theory and Techniques*, vol. 48, no. 11, pp. 1841–53, Nov. 2000.

[6] J. E. Bridges, "Non-invasive system for breast cancer detection," U.S. Patent No. 5,704,355, Jan. 1998.

[7] J. E. Bridges, "Breast cancer detection, imaging and screening by electromagnetic millimeter waves," U.S. Patent No. 5,807,257, Sept. 1998.

[8] J. E. Bridges, "Microwave method and system to detect and locate cancer in heterogeneous tissues," U.S. Patent No. 5,829,437, Nov. 1998.

[9] J. E. Bridges, A. Taflove, S. C. Hagness, and A. Sahakian, "Microwave antenna for cancer detection system," U.S. Patent application submitted Sept 9, 1997.

[10] M. Popovic, S. C. Hagness, A. Taflove, and J. E. Bridges, "2-D FDTD study of a fixed-focus elliptical reflector system for breast cancer detection: frequency window for optimum operation," paper AP76-8 in *Proc. 1998 IEEE Antennas and Propagation Society Int. Symp.* Atlanta, GA, June 21 – 26, 1998.

[11] S. C. Hagness, A. Taflove, and J. E. Bridges, "FDTD analysis of a pulsed microwave confocal system for breast cancer detection," in *Proc. 19th Int. Conf. IEEE Engineering in Medicine and Biology Society,* Chicago, IL, Oct. 30 – Nov 2, 1997, pp. 2506 – 2508.

[12] S. C. Hagness, A. Taflove, and J. E. Bridges, "FDTD modeling of a coherent-addition antenna array for early-stage detection of breast cancer," paper AP45-7 in *Proc. 1998 IEEE Antennas and Propagation Society Int. Symp.* Atlanta, GA, June 21 – 26, 1998.

[13] M. Wickman, "Breast reconstruction – past achievements, current status and future goals," *Scandinavian Journal of Plastic and Reconstructive and Hand Surgery*, vol. 29, pp. 81–100, 1995.

[14] M. Wickman, Goran Jurell, and Kerstin Sandelin, "Immediate breast reconstruction: short term experience in 75 consecutive cases," *Scandinavian Journal of Plastic and Reconstructive and Hand Surgery*, vol. 29, pp. 153–159, 1995.

[15] M. Olenius and O. Johansson, "Variations in epidermal thickness in expanded human breast skin," *Scandinavian Journal of Plastic and Reconstructive and Hand Surgery*, vol. 29, pp. 15–20, 1995.

[16] Jr. T. L. Pope, M. E. Read, T. Medsker, A. J. Buschi, and A. N. Brenbridge, "Breast skin thickness: normal range and causes of thickening shown on film-screen mammography," *Journal of the Canadian Association of Radiologists*, vol. 35, pp. 365–368, Dec. 1984.

[17] S. S. Chaudhary, R. K. Mishra, A. Swarup, and J. M. Thomas, "Dielectric properties of normal and malignant human breast tissues at radiowave and microwave frequencies," *Indian Journal of Biochemistry and Biophysics*, vol. 21, pp. 76–79, 1984.

[18] C. C. Johnson and A. W. Guy, "Nonionizing electromagnetic wave effects in biological materials and systems," *IEEE Proceedings*, vol. 60, pp. 694, 1972.

[19] C. Gabriel, S. Gabriel, and E. Corthout, "The dielectric properties of biological tissues: I. literature survey," *Physics in Medicine and Biology*, vol. 41, no. 11, pp. 2231–2249, Nov. 1996.

[20] S. Gabriel, R. W. Lau, and C. Gabriel, "The dielectric properties of biological tissues: II. measurements on the frequency range 10 Hz to 20 GHz," *Physics in Medicine and Biology*, vol. 41, no. 11, pp. 2251–2269, Nov. 1996.

[21] S. Gabriel, R. W. Lau, and C. Gabriel, "The dielectric properties of biological tissues: III. Parametric models for the dielectric spectrum of tissues," *Physics in Medicine and Biology*, vol. 41, no. 11, pp. 2271–2293, Nov. 1996.

[22] J. P. Grant, R. N. Clarke, G. T. Symm, and N. M Spyrou, "*in vivo* dielectric properties of human skin from 50 mhz to 2.0 ghz," *Physics in Medicine and Biology*, vol. 33, no. 5, pp. 607–612, 1988.

[23] J. Ch. Bolomey, D. Lesselier, C.Pichot, and W. Tabbara, "Spectral and time domain approaches to some inverse scattering problems," *IEEE Transactions on Antennas and Propagation*, vol. 29, no. 2, pp. 206–212, 1981.

[24] S. Coen, K. K. Mei, and D. J. Anelakos, "Inverse scattering technique applies to remote sensing of layered media," *IEEE Transactions on Antennas and Propagation*, vol. 29, no. 2, pp. 298–306, 1981.

[25] W. Tabbara, "Reconstruction of permittivity profiles from a spectral analysis of the reflection coefficient," *IEEE Transactions on Antennas and Propagation*, vol. 27, no. 2, pp. 241–244, 1979.

[26] M. Mostafavi and R. Mittra, "Remote probing of inhomogeneous media using parameter optimization techniques," *Radio Science*, vol. 7, no. 12, pp. 1105–1111, 1972.

[27] C. J. Leuschen and R. G. Plumb, "A matched-filter-based reverse-time migration algorithm for ground-penetrating radar data," *IEEE Transactions on Geoscience and Remote Sensing*, vol. 39, no. 5, pp. 929–936, May 2001.

[28] J. F. Ma, W. H. Yu, and R. Mittra, "Detection of buried dielectric cavities using the finite-difference time-domain method in conjunction with signal processing techniques," *IEEE Transactions on Antennas and Propagation*, vol. 48, no. 9, pp. 1289–1294, Sept. 2000.

[29] A. Qing, C. K. Lee, and L. Jen, "Electromagnetic inverse scattering of two-dimensional perfectly conducting objects by real-coded genetic algorithm," *IEEE Transactions on Geoscience and Remote Sensing*, vol. 39, no. 3, pp. 665–676, Mar. 2001.

[30] K. R. Umashankar, S. Chaudhuri, and A. Taflove, "Finite-difference time-domain formulation of an inverse scattering scheme for remote sensing of inhomogeneous lossy layered media," *Journal of Electromagnetic Waves and Applications*, vol. 8, pp. 489–509, 1994.

[31] M. A. Strickel, A. Taflove, and K. R. Umashankar, "Finite-difference time-domain formulation of an inverse scattering scheme for remote sensing of conducting and dielectric targets," *Journal of Electromagnetic Waves and Applications*, vol. 8, pp. 510–529, 1994.

TABLES AND FIGURES

Fig. 1. Geometry showing the antenna array adjacent to the skin and the path used for estimating propagation time delays for a $5-mm$ tumor embedded in the breast tissue 3 cm from the skin surface. Both breast and skin tissue are considered to be homogeneous with $\varepsilon_{r-breast} = 9$ and $\varepsilon_{r-skin} = 36$.

Fig. 2. Effect of skin thickness on propagation time delays for each antenna element of Fig. 1, assuming $\varepsilon_{r-skin} = 36$. Reported range of normal skin thickness is $0.5 - 2.7\ mm$.

Fig. 3. Time-domain inverse-scattering iterative algorithm for recovery of dielectric parameters ε_r and σ from a measured (in this study, simulated measured) signal. The scheme exploits causality to limit the region of inversion.

Fig. 4. Inverse-scattering FDTD computation for a skin half-space: (a) Convergence of ε_{r-skin} to its correct value of 36 for two different initial guesses of ε_{r-skin}, with σ_{skin} fixed at the correct value of 4 S/m . (b) Convergence of σ_{skin} to its correct value of 4 S/m for two different initial guesses of σ_{skin}, with ε_{r-skin} fixed at the correct value of 36 .

Fig. 5. Estimate of ε_{r-skin} for trial values of σ_{skin} for the $120-ps$ differentiated Gaussian pulse excitation case. (a) Search trajectory in $(\varepsilon_{r-skin}, \sigma_{skin})$ space for $T_{window} = 400\Delta t$ and $T_{window} = 600\Delta t$, where $\Delta t = 0.33356\ ps$. (b) Error vs. trial values of σ_{skin} for $T_{window} = 400\Delta t$.

Fig. 6. Estimate of σ_{skin} for trial values of ε_{r-skin} for the $120-ps$ differentiated Gaussian pulse excitation. (a) Search trajectory in $(\varepsilon_{r-skin}, \sigma_{skin})$ space for $T_{window} = 400\Delta t$, where $\Delta t = 0.33356\,ps$. (b) Error vs. estimated σ_{skin} values, showing a broad null at the location of the assumed reference values of the skin parameters.

Fig. 7. Estimate of σ_{skin} for trial values of ε_{r-skin} for the $5-ps$ rise-time ramp excitation. (a) Search trajectory in $(\varepsilon_{r-skin}, \sigma_{skin})$ space for $T_{window} = 100\Delta t$, where $\Delta t = 0.33356\,ps$.

(b) Error vs. estimated σ_{skin} values, showing a broad null at the location of the assumed reference values of the skin parameters.

Fig. 8. Estimate of σ_{skin} for trial values of ε_{r-skin} for the $10-ps$ differentiated Gaussian pulse excitation. (a) Search trajectory in $(\varepsilon_{r-skin}, \sigma_{skin})$ space for $T_{window} = 80\Delta t$, where $\Delta t = 0.33356\,ps$. (b) Error vs. estimated σ_{skin} values, showing a sharp null at the location of the assumed reference values of the skin parameters.

Fig. 9. (a) Sample trajectories in the $(\varepsilon_{r-skin}, \sigma_{skin})$ space for the $10-ps$ differentiated Gaussian pulse excitation with $S/N = 20\ dB$. (b) Error vs. estimated σ_{skin} values for the averaged-backscattered-waveform case.

Fig. 10. (a) Sample trajectories in the $(\varepsilon_{r-skin}, \sigma_{skin})$ space for the $10-ps$ differentiated Gaussian pulse excitation with $S/N = 40\ dB$. (b) Error vs. estimated σ_{skin} values for the averaged-backscattered-waveform case.

Fig. 11. Waveforms illustrating a strategy for estimating the skin thickness making use of the previously determined values of ε_{r-skin} and σ_{skin}. We compare the simulated measured response (magnetic field component at the location of the antenna) for four finite skin-thickness cases with a simulation which assumes a homogeneous skin half-space.

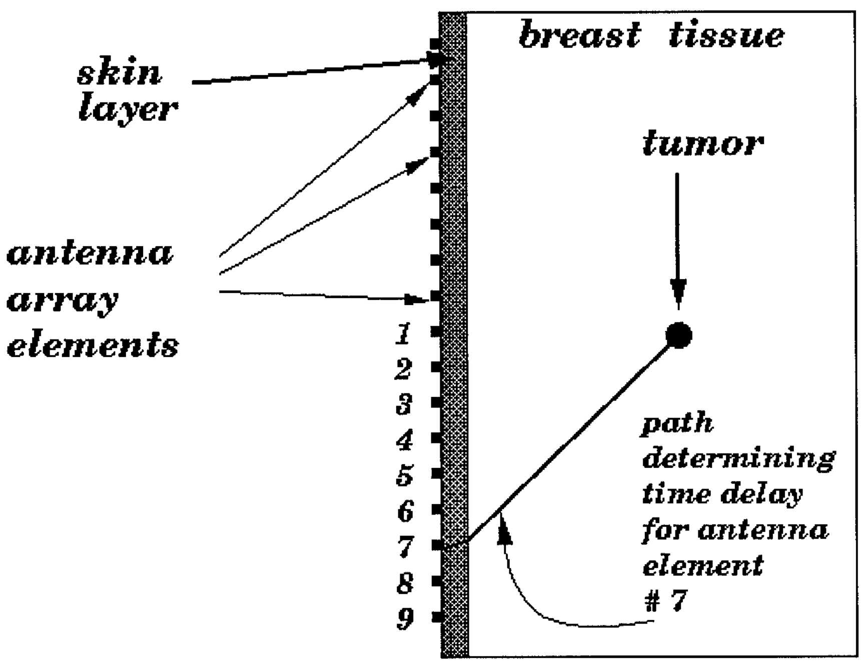
breast tissue
skin
layer
tumor
antenna
array
elements
1
2
3
4
5
6
7
8
9
path
determining
time delay
for antenna
element
7

Fig. 1

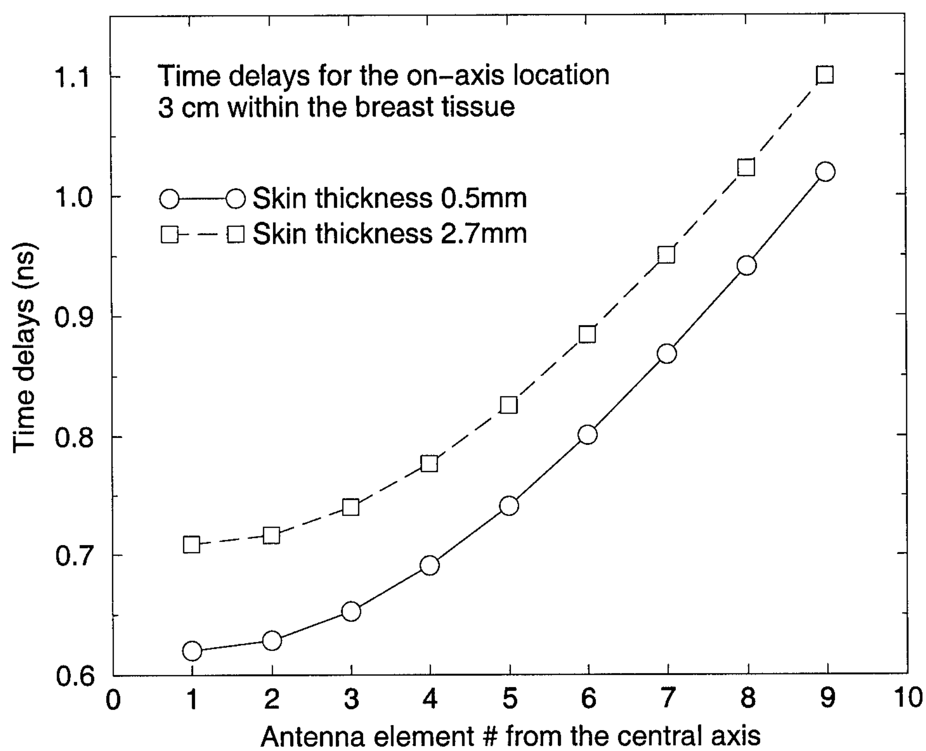
Time delays for the on–axis location
3 cm within the breast tissue
Skin thickness 0.5mm
Skin thickness 2.7mm
Time delays (ns)
0.6
0.7
0.8
0.9
1.0
1.1
0
1
2
3
4
5
6
7
8
9
10
Antenna element # from the central axis

Fig. 2

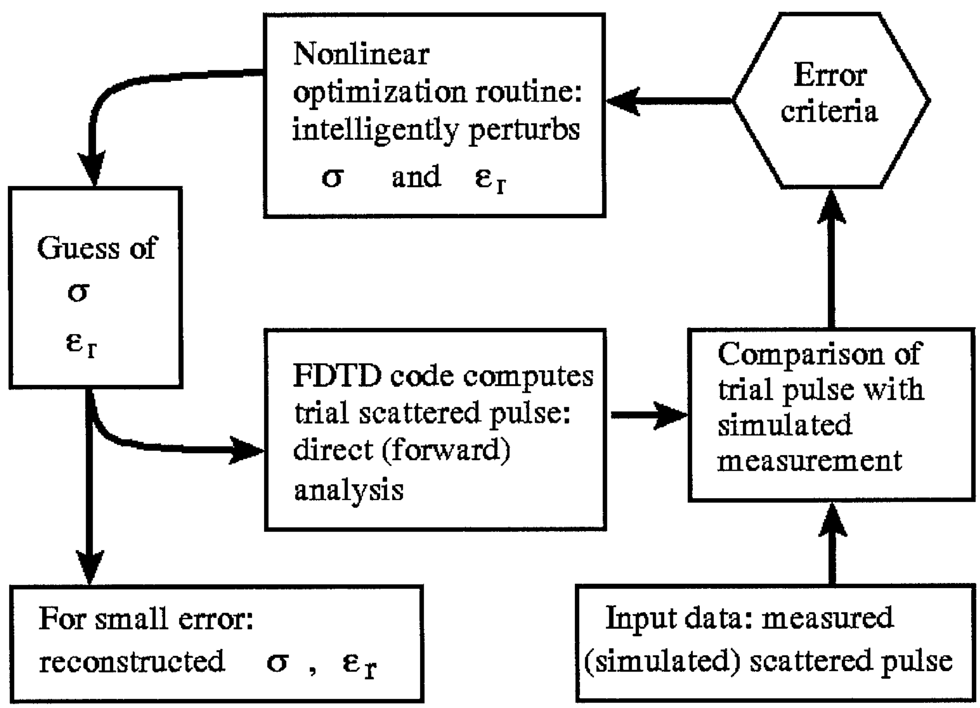
Nonlinear
optimization routine:
intelligently perturbs
σ and ε_r
Error
criteria
Guess of
σ
ε_r
FDTD code computes
trial scattered pulse:
direct (forward)
analysis
Comparison of
trial pulse with
simulated
measurement
For small error:
reconstructed σ , ε_r
Input data: measured
(simulated) scattered pulse

Fig. 3

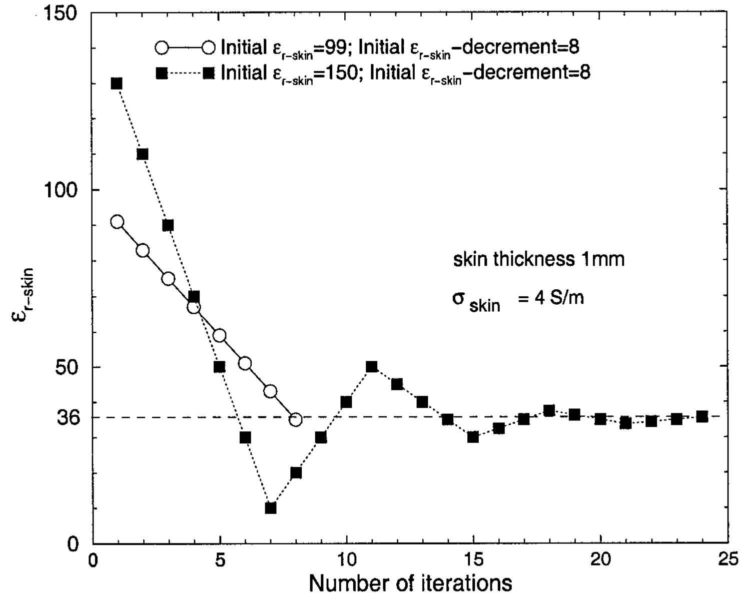
Initial ε_{r-skin}=99; Initial ε_{r-skin}-decrement=8
Initial ε_{r-skin}=150; Initial ε_{r-skin}-decrement=8
skin thickness 1mm
σ_{skin} = 4 S/m
ε_{r-skin}
Number of iterations

(a)

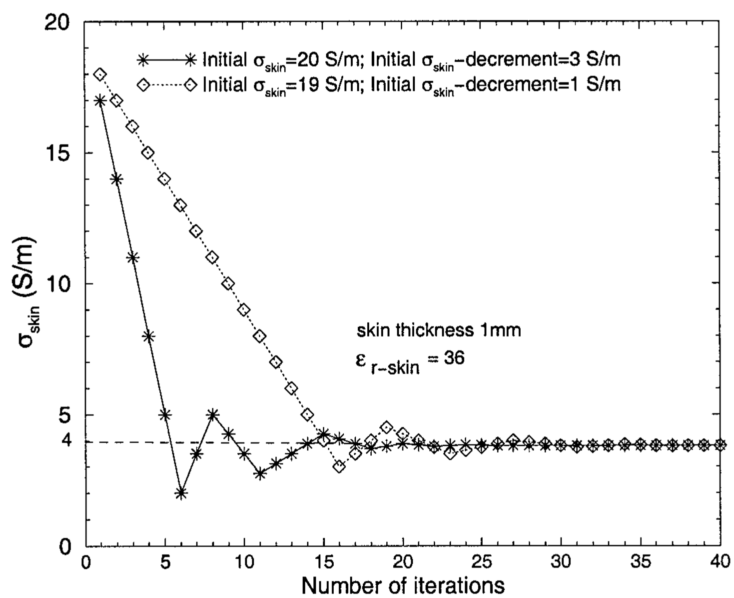
Initial σ_{skin}=20 S/m; Initial σ_{skin}-decrement=3 S/m
Initial σ_{skin}=19 S/m; Initial σ_{skin}-decrement=1 S/m
skin thickness 1mm
ε_{r-skin} = 36
σ_{skin} (S/m)
Number of iterations

(b)

Fig. 4

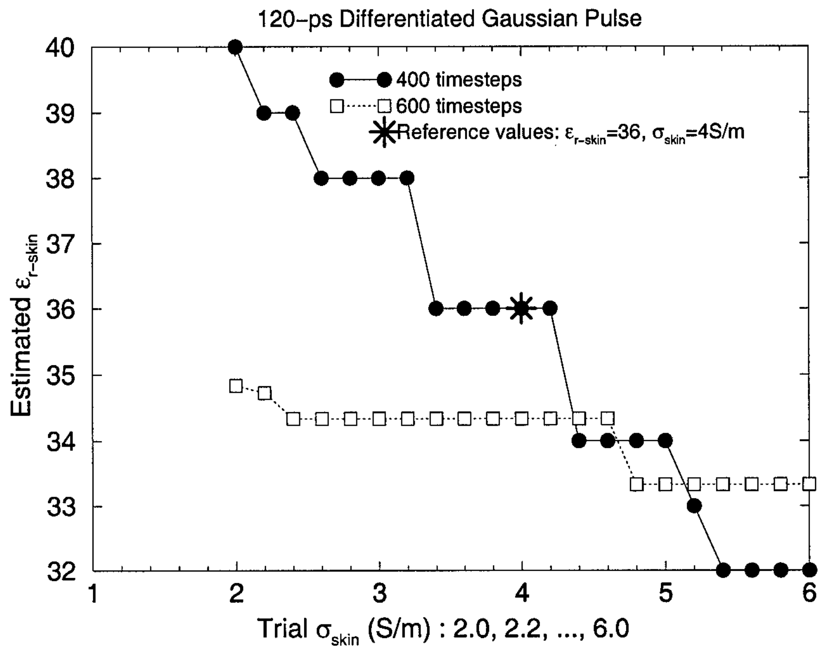
120-ps Differentiated Gaussian Pulse
400 timesteps
600 timesteps
Reference values: $\varepsilon_{r\text{-skin}}$=36, σ_{skin}=4S/m
Estimated $\varepsilon_{r\text{-skin}}$
Trial σ_{skin} (S/m) : 2.0, 2.2, ..., 6.0

(a)

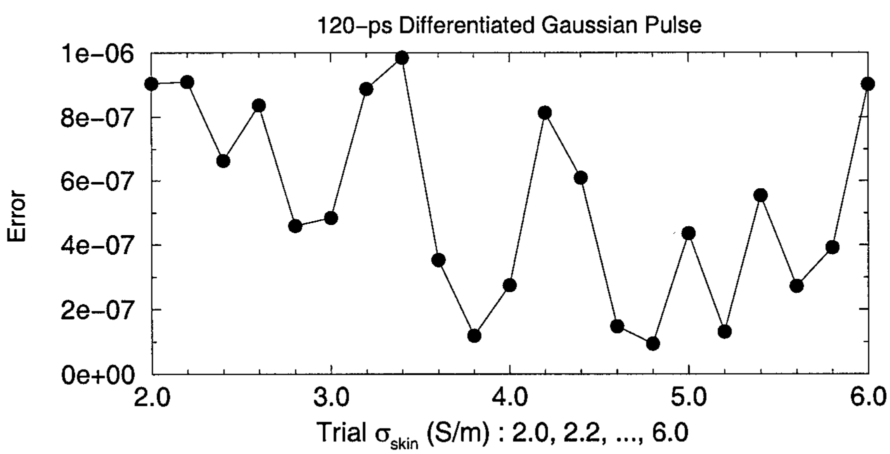
120-ps Differentiated Gaussian Pulse
Error
Trial σ_{skin} (S/m) : 2.0, 2.2, ..., 6.0

(b)

Fig. 5

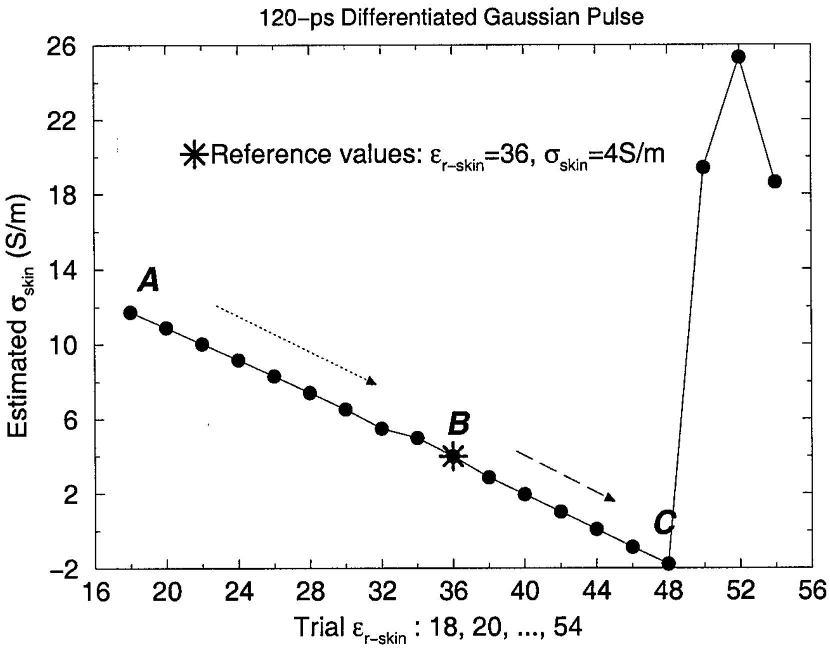
120-ps Differentiated Gaussian Pulse
Reference values: ε_{r-skin}=36, σ_{skin}=4S/m
Estimated σ_{skin} (S/m)
Trial ε_{r-skin} : 18, 20, ..., 54
A
B
C

(a)

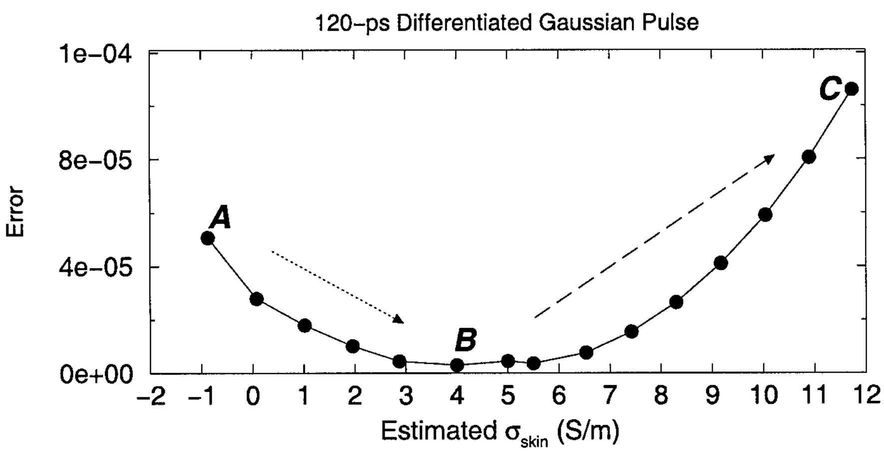
120-ps Differentiated Gaussian Pulse
Error
Estimated σ_{skin} (S/m)
A
B
C

(b)

Fig. 6

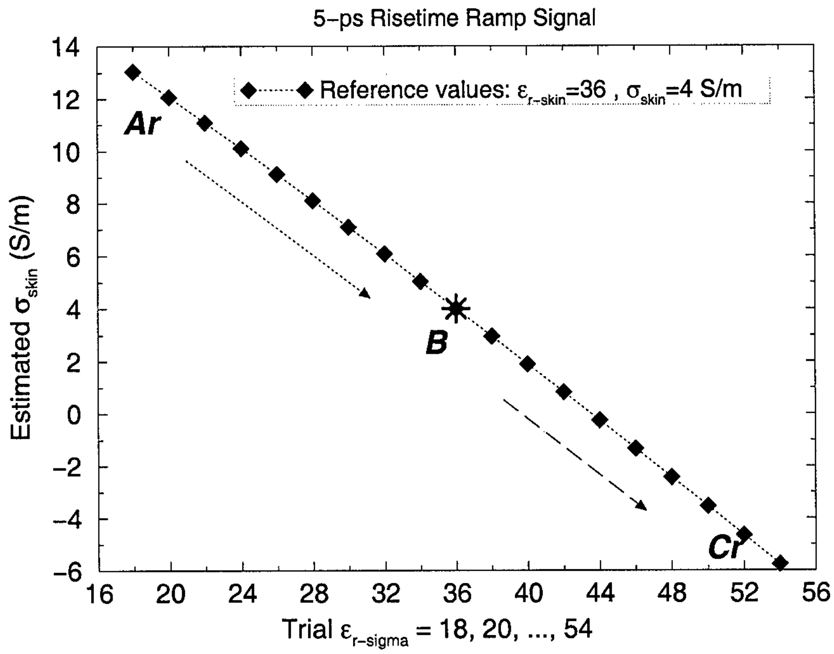
5-ps Risetime Ramp Signal
Reference values: $\varepsilon_{r\text{-skin}}$=36 , σ_{skin}=4 S/m
Estimated σ_{skin} (S/m)
Trial $\varepsilon_{r\text{-sigma}}$ = 18, 20, ..., 54
Ar
B
Cr
14
12
10
8
6
4
2
0
-2
-4
-6
16
20
24
28
32
36
40
44
48
52
56

(a)

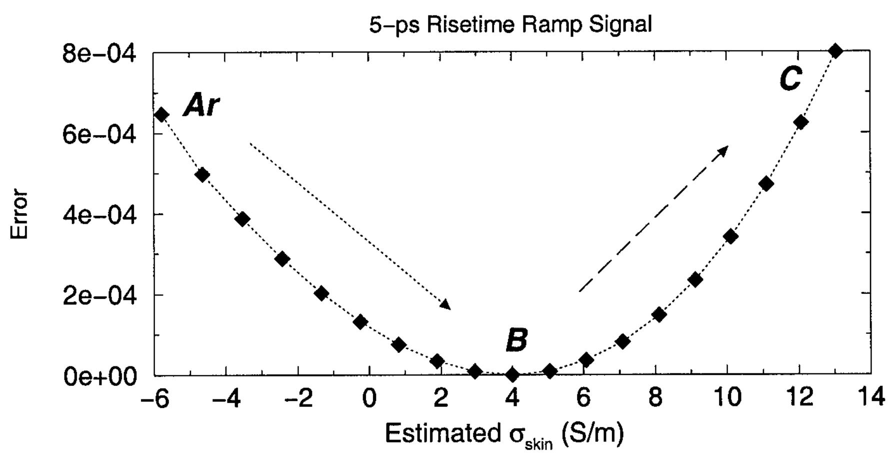
5-ps Risetime Ramp Signal
Error
Estimated σ_{skin} (S/m)
Ar
B
C
8e-04
6e-04
4e-04
2e-04
0e+00
-6
-4
-2
0
2
4
6
8
10
12
14

(b)

Fig. 7

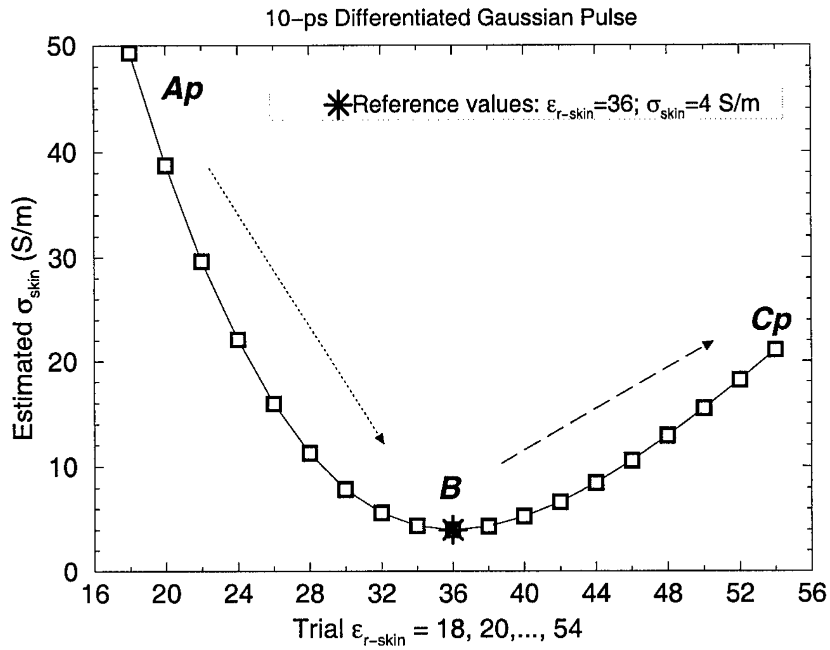
10-ps Differentiated Gaussian Pulse
Reference values: $\varepsilon_{r\text{-skin}}$=36; σ_{skin}=4 S/m
Ap
B
Cp
Estimated σ_{skin} (S/m)
Trial $\varepsilon_{r\text{-skin}}$ = 18, 20,..., 54
0
10
20
30
40
50
16
20
24
28
32
36
40
44
48
52
56

(a)

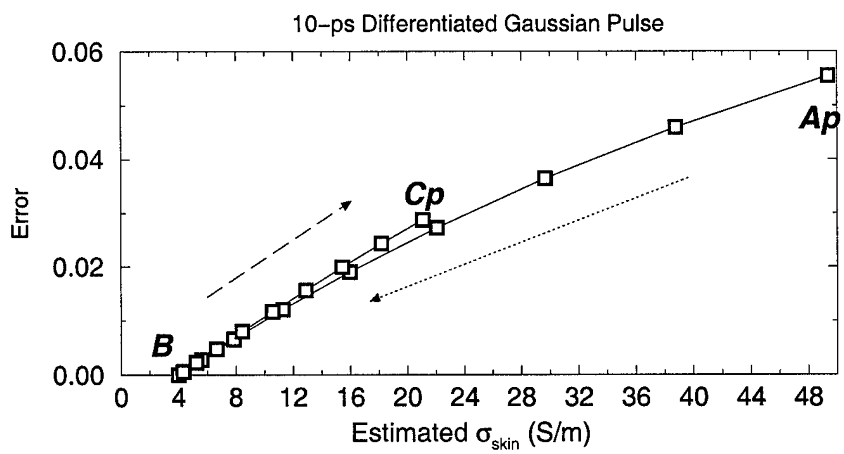
10-ps Differentiated Gaussian Pulse
Ap
Cp
B
Error
Estimated σ_{skin} (S/m)
0.00
0.02
0.04
0.06
0
4
8
12
16
20
24
28
32
36
40
44
48

(b)

Fig. 8

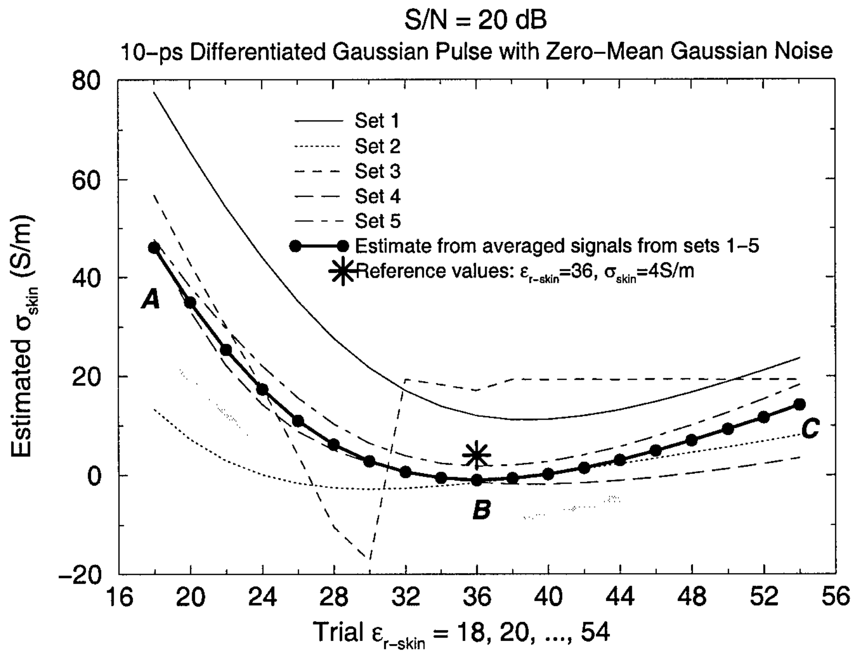

S/N = 20 dB
10–ps Differentiated Gaussian Pulse with Zero–Mean Gaussian Noise
Set 1
Set 2
Set 3
Set 4
Set 5
Estimate from averaged signals from sets 1–5
Reference values: $\varepsilon_{r\text{-skin}}$=36, σ_{skin}=4S/m
A
B
C
Estimated σ_{skin} (S/m)
Trial $\varepsilon_{r\text{-skin}}$ = 18, 20, ..., 54

(a)

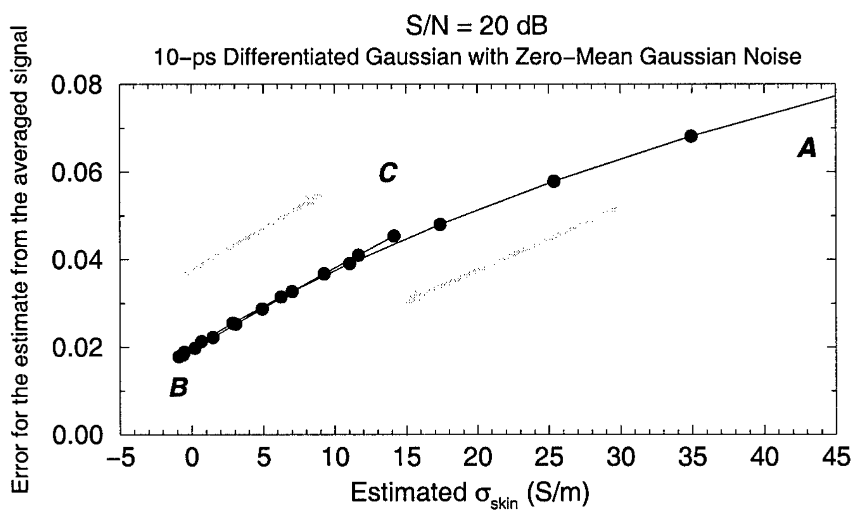

S/N = 20 dB
10–ps Differentiated Gaussian with Zero–Mean Gaussian Noise
A
B
C
Error for the estimate from the averaged signal
Estimated σ_{skin} (S/m)

(b)

Fig. 9

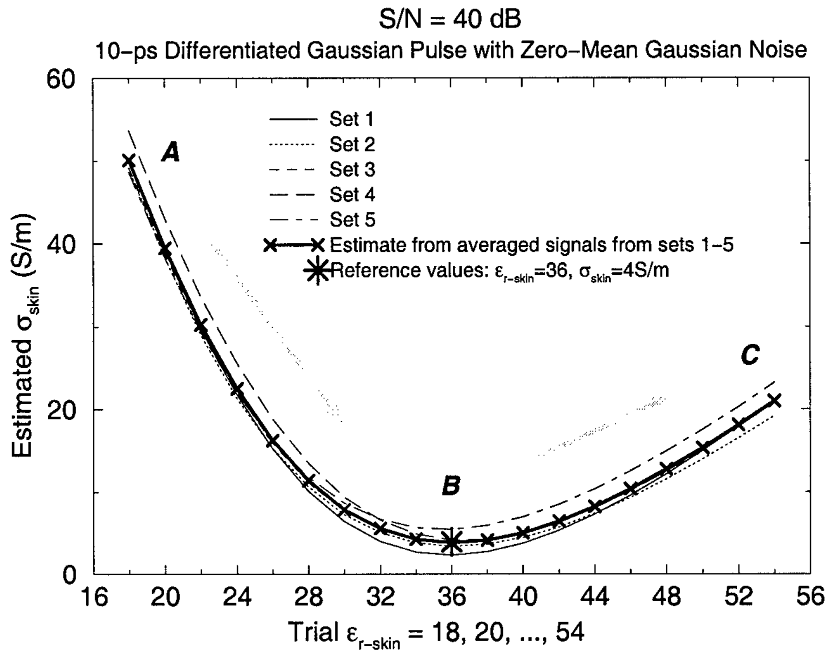
S/N = 40 dB
10-ps Differentiated Gaussian Pulse with Zero-Mean Gaussian Noise
Set 1
Set 2
Set 3
Set 4
Set 5
Estimate from averaged signals from sets 1-5
Reference values: $\varepsilon_{r\text{-skin}}$=36, σ_{skin}=4S/m
A
B
C
Estimated σ_{skin} (S/m)
Trial $\varepsilon_{r\text{-skin}}$ = 18, 20, ..., 54

(a)

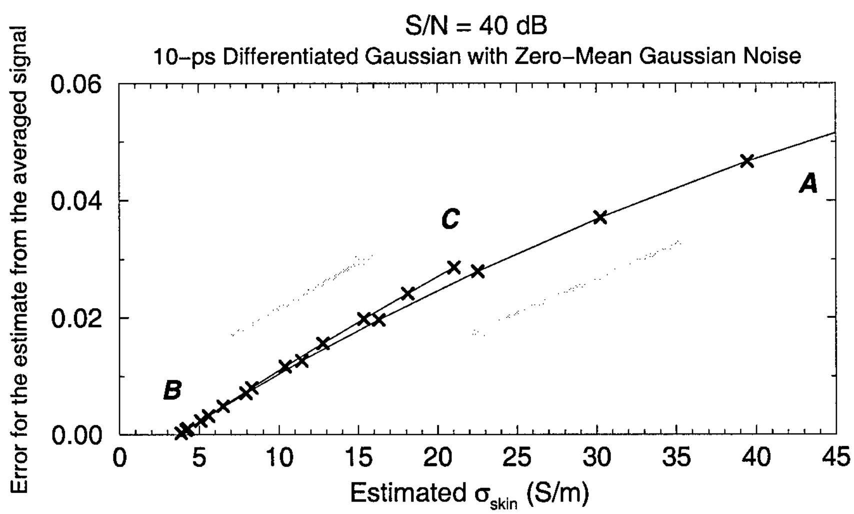
S/N = 40 dB
10-ps Differentiated Gaussian with Zero-Mean Gaussian Noise
A
B
C
Error for the estimate from the averaged signal
Estimated σ_{skin} (S/m)

(b)

Fig. 10

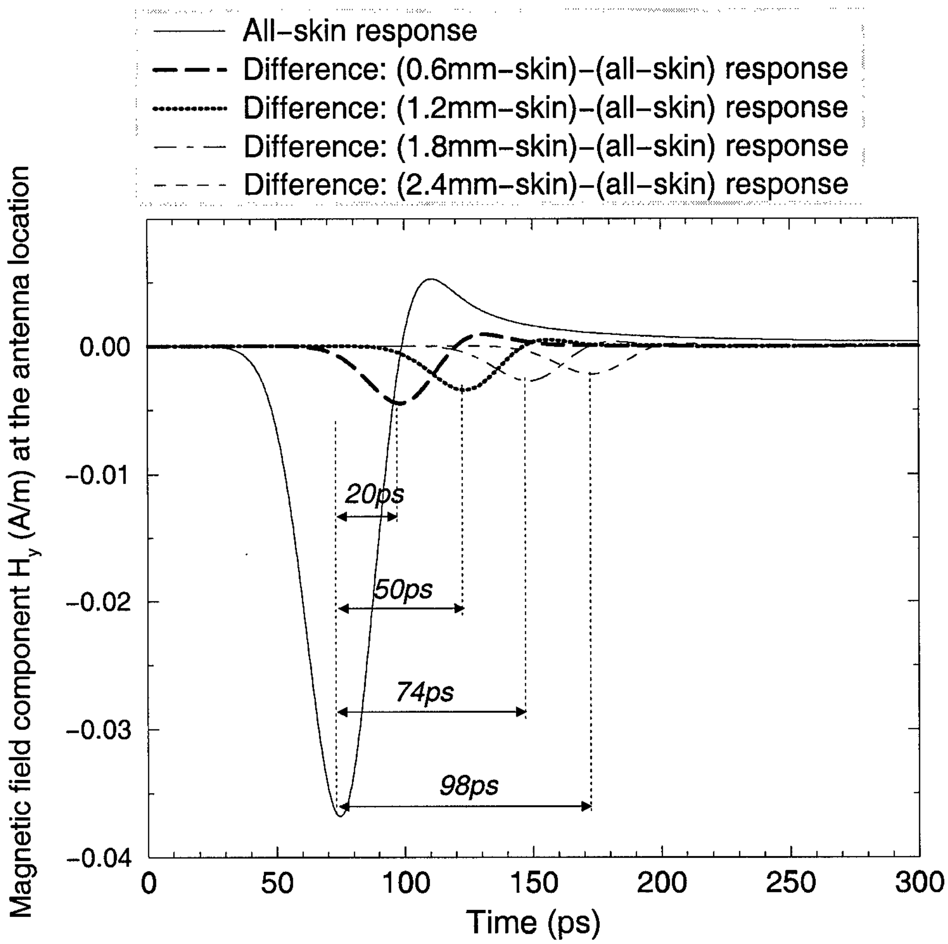

All–skin response
Difference: (0.6mm–skin)–(all–skin) response
Difference: (1.2mm–skin)–(all–skin) response
Difference: (1.8mm–skin)–(all–skin) response
Difference: (2.4mm–skin)–(all–skin) response
Magnetic field component H_y (A/m) at the antenna location
0.00
−0.01
−0.02
−0.03
−0.04
20ps
50ps
74ps
98ps
0
50
100
150
200
250
300
Time (ps)

Fig. 11

Appendix B

Conference digests / abstracts for 2002.

Conference abstract: for the Bioelectromagnetics Society 24th Annual Meeting, June 23-27, 2002, Quebec City, Canada.

2-D FDTD INVERSE-SCATTERING SCHEME FOR DETERMINING MICROWAVE BREAST SKIN PROPERTIES: THE RESULTS AND THE IMPLIED OPTIMIZATION OPTIONS. M. Popović[1] , A. Taflove[2*]. [1] Department of Electrical and Computer Engineering, McGill University, Montréal, Quebec, Canada H3A 2A7. [2] Electrical and Computer Engineering Department, Northwestern University, Evanston, Illinois 60208, USA.

Introduction: The work reported in this paper is motivated by the development of a new confocal microwave technology to detect and image early-stage breast cancers. This methodology depends upon knowledge of the average dielectric properties of the local breast tissues. Patient-specific calibration of the microwave imager requires knowledge of these properties. Present results focus on dielectric properties and thickness of skin in the area of human breast. Well-documented findings have shown that skin thickness varies from patient to patient and also with location on the body of an individual patient.

Objective: A three-dimensional (3-D) inverse-scattering finite-difference time-domain (FDTD) algorithm would permit non-invasive measurement of near-surface breast tissue dielectric properties, based on the information contained in the backscattered signal recorded with a trans-receiving antenna located on the skin surface. Initial investigations are done in two dimensions. Development of a two-dimensional (2-D) FDTD algorithm allows for study of the inverse-scattering scheme and the possibilities for its optimization with a computational cost lower than that of the 3-D numerical investigations.

Methods: A 2-D inverse-scattering algorithm based upon the FDTD method is presented for determining skin thickness and the relative permittivity $\varepsilon_{r\text{-}skin}$ and electric conductivity σ_{skin} in the microwave range. This scheme applies an iterative technique to the case of a 2-D half-space excited at its surface by an infinitely long monopole. The algorithm traces a search trajectory in the $(\varepsilon_{r\text{-}skin}, \sigma_{skin})$ parameter space in the following manner. A trial value of σ_{skin} is assumed and a series of FDTD forward-scattering runs is conducted to find a corresponding value of $\varepsilon_{r\text{-}skin}$ which minimizes the energy-normed error relative to the measured backscattered signal. This procedure is then repeated for a sequence of trial values of σ_{skin} which vary uniformly in equal increments within a ±50% range about the nominal value reported in the literature. The three electric-field excitation waveforms used for the dielectric parameter reconstruction are as follows: (a) 120-ps differentiated Gaussian pulse; (b) 10-ps differentiated Gaussian pulse with a 5-ps rise-time; and (c) 5-ps rise-time ramp which has the same maximum as the peak value of the 10-ps differentiated Gaussian pulse. The robustness of the inverse-scattering scheme was tested by adding zero-mean Gaussian noise to the simulated measured backscattered signals for signal-to-noise ratios of 20dB and 40dB.

Results and Conclusions: There are two significant findings of this work. (1) The use of a time-linear (ramp) excitation yields a linear search trajectory in the $(\varepsilon_{r\text{-}skin}, \sigma_{skin})$ parameter space. (2) The use of a short bipolar excitation signal provides a sharp null of the energy-normed error along the search trajectory even when the backscattered signal is contaminated with a significant level of additive zero-mean Gaussian noise. Proper combination of time-linear and short bipolar pulse excitation data can yield an efficient and robust search strategy.

This work was sponsored by the United States Department of Defense pre-doctoral grant, under Army Award number DAMD17-99-1-9335. The authors would like to thank Cray Research for their computational resources.

Conference digest for: The Tenth Biennial IEEE Conference on Electromagnetic Field Computation, (CEFC2002), June 16-19, 2002, Perugia, Italy.

Noninvasive Measurement of Breast Skin Properties in the Microwave Range: Efficiency Improvement of the 2-D FDTD Inverse-Scattering Scheme

Prof. Milica Popović
Department of Electrical and Computer Engineering
McGill University
3480 University Street, Montréal, Québec, CANADA H3A 2A7
Email: poppy@ece.mcgill.ca

Prof. Allen Taflove
Electrical and Computer Engineering Department
Northwestern University
2145 Sheridan Road, Evanston, Illinois 60208, USA

***Abstract* – We investigate a two-dimensional FDTD inverse-scattering technique for noninvasive determination of breast skin properties. Convergence of the algorithm depends on the shape and the duration of the excitation waveform. Efficiency and robustness of this scheme are improved by a proper combination of time-linear and short bipolar pulse excitation.**

I. Introduction and Background

Our work is motivated by the need for patient-specific calibration of recently proposed systems [1] for microwave breast cancer detection. To obtain the tumor image within the breast, the signals received by a trans-receiving antenna array contacting the breast are summed coherently with a digital-processing scheme which assumes knowledge of the average dielectric properties of the local breast tissues. These properties (relative permittivity $\varepsilon_{r\text{-skin}}$, conductivity σ_{skin} and skin thickness) vary from patient to patient as well as with location within the breast area within an individual.

II. Methods

Numerical method. In order to develop an inverse-scattering algorithm which would permit noninvasive measurement of breast skin properties, we first investigate a two-dimensional (2-D) time-domain technique based upon an FDTD forward-scattering program element embedded within a numerical feedback error-minimization loop. The one-dimensional inversion technique of [2] is extended to 2-D illumination of a layered medium by an infinite monopole source located at the surface.

Simultaneous recovery of the parameters. The scheme generates a search trajectory in the ($\varepsilon_{r\text{-skin}}$, σ_{skin}) space in the following manner. A trial value of $\varepsilon_{r\text{-skin}}$ is assumed. A series of FDTD forward-scattering runs is conducted to find a corresponding value of σ_{skin} which minimizes the energy-normed error relative to the measured backscattered signal. This procedure is repeated for a sequence of trial $\varepsilon_{r\text{-skin}}$ values which vary uniformly in equal increments within a ±50% range about the nominal value reported in the literature.

Excitation waveforms. The time waveform and the duration of the illuminating pulse are studied to explore convergence optimization of the inverse-scattering technique. Among the E_z-field excitation waveforms under investigation were: (a) 10-ps differentiated Gaussian pulse with a 5-ps rise time; and (b) 5-ps rise time ramp.

III. Results and Discussion

It is shown that the convergence of the inverse-scattering technique depends on the shape and the duration of the illuminating electromagnetic wave pulse chosen for the electric parameter reconstruction. For the 5-ps rise time ramp, the search trajectory in the ($\varepsilon_{r\text{-skin}}$, σ_{skin}) space exhibits linear behavior; the error along the search trajectory has a broad null. In the case of the 10-ps differentiated Gaussian pulse (where the time window of inversion includes the entire bipolar backscattered waveform) the search trajectory shows parabolic behavior; the error along the search trajectory has a sharp null at the location of the assumed reference values of the skin dielectric parameters, which suggests robustness of parameter recovery in the presence of noise.

For the 5-ps ramp excitation waveform, it can be shown that the linearity of the search trajectory in the ($\varepsilon_{r\text{-skin}}$, σ_{skin}) space follows from the time linearity of the excitation signal and the condition of the minimal error condition. The potential benefit of this linearity is as follows: linear excitation can be used for two trial $\varepsilon_{r\text{-skin}}$ values, and the rest of the values along the anticipated ($\varepsilon_{r\text{-skin}}$, σ_{skin}) trajectory can be obtained by interpolation or extrapolation. Then, error values for the sets of ($\varepsilon_{r\text{-skin}}$, σ_{skin}) obtained by this means can be tested with the noise-robust 10-ps differentiated Gaussian pulse excitation. This would significantly decrease the computational cost of the dielectric recovery procedure.

This work was sponsored by the US DOD pre-doctoral grant (Award Number DAMD17-99-1-9335).

[1] E. C. Fear and M. A. Stuchly, "Microwave detection of breast cancer, " *IEEE Trans. on Microwave Theory and Techniques*, vol. 48, no 11, pp 1854-63, Nov. 2000.

[2] K. R. Umashankar, S. Chauhuri and A. Taflove, "Finite-difference time-domain formulation of an inverse scattering scheme for remote sensing of inhomogeneous lossy layered media,", *J. of Electromagnetic Waves and Apps.* ,vol. 8, pp. 489-509, 1994.

Appendix C

Material related to investigator's Doctoral Degree.

THE GRADUATE SCHOOL

This is to certify that

MILICA POPOVIC

has completed all requirements for the degree

DOCTOR OF PHILOSOPHY

to be formally awarded

DECEMBER 28, 2001

August 1, 2001
Date

Lawrence J. Henschen
Associate Dean

NORTHWESTERN UNIVERSITY

NORTHWESTERN UNIVERSITY

Microwave Imaging of Breast Tissues

A DISSERTATION

SUBMITTED TO THE GRADUATE SCHOOL

IN PARTIAL FULFILLMENT OF THE REQUIREMENTS

for the degree

DOCTOR OF PHILOSOPHY

Field of Electrical and Computer Engineering

By

Milica Popović

EVANSTON, ILLINOIS

December 2001

Appendix D

Copy of letter of appointment for investigator's employment as an assistant professor at McGill University.

McGill

Luc Vinet

Vice-Principal (Academic)
McGill University
James Administration Building
845 Sherbrooke Street West
Montréal, QC, Canada H3A 2T5

Vice-principal (enseignement)
Université McGill
Pavillon James de l'administration
845, rue Sherbrooke ouest
Montréal, (Québec) Canada H3A 2T5

Tel: (514) 398-3331
Fax/Télécopieur: (514) 398-3219
E-MAIL: VINET@VPA.MCGILL.CA

August 8, 2001

Dr. Milica Popovic
Dept. of Electrical & Computer Engineering
McConnell Engineering Bldg.

Dear Dr. Popovic:

On behalf of the Board of Governors of McGill University, I write to inform you that you are appointed full-time tenure-track Assistant Professor in the Department of Electrical and Computer Engineering, Faculty of Engineering, for the term beginning **September 1, 2001** and ending **August 31, 2004**.

This letter of appointment and the Regulations of the University, including the Regulations Relating to the Employment of Academic Staff as modified by the Board of Governors from time to time, form your contract with the University and no modification thereto has any validity unless approved by the Board of Governors.

In accordance with Canadian and Québec law, this appointment is conditional on your obtaining the appropriate authorization to work from Citizenship and Immigration Canada, Immigration Québec and, if applicable, Human Resources and Development Canada.

I welcome you to the McGill community and express the hope that you will enjoy your responsibilities at the University.

Sincerely,

Luc Vinet

Luc Vinet
Provost and Vice-Principal (Academic)

LV/mfo

cc: Dean, Faculty of Engineering
Records & Systems, HR

The McGill Handbook of Regulations and Policies for Academic Staff is available on the Secretariat website:
http://www.mcgill.ca/Secretariat